Annual Review of Marine Science

Using Chlorophyll Fluorescence to Determine the Fate of Photons Absorbed by Phytoplankton in the World's Oceans

Maxim Y. Gorbunov and Paul G. Falkowski

Environmental Biophysics and Molecular Ecology Program, Department of Marine and Coastal Sciences, Rutgers, The State University of New Jersey, New Brunswick, New Jersey 08901, USA; email: gorbunov@marine.rutgers.edu, falko@marine.rutgers.edu

Annu. Rev. Mar. Sci. 2022. 14:213–38

First published as a Review in Advance on August 30, 2021

The *Annual Review of Marine Science* is online at marine.annualreviews.org

https://doi.org/10.1146/annurev-marine-032621-122346

Keywords

variable fluorescence, photosynthesis, fluorescence lifetime

Abstract

Approximately 45% of the photosynthetically fixed carbon on Earth occurs in the oceans in phytoplankton, which account for less than 1% of the world's photosynthetic biomass. This amazing empirical observation implies a very high photosynthetic energy conversion efficiency, but how efficiently is the solar energy actually used? The photon energy budget of photosynthesis can be divided into three terms: the quantum yields of photochemistry, fluorescence, and heat. Measuring two of these three processes closes the energy budget. The development of ultrasensitive, seagoing chlorophyll variable fluorescence and picosecond fluorescence lifetime instruments has allowed independent closure on the first two terms. With this closure, we can understand how phytoplankton respond to nutrient supplies on timescales of hours to months and, over longer timescales, to changes in climate.

HISTORICAL PERSPECTIVE

In 1834, Sir David Brewster, a Scottish scientist who was fascinated by light and had invented the kaleidoscope 20 years earlier, reported that when absolute alcohol extracts of laurel leaves were exposed to blue light (which was obtained using a prism), three *red* (his italics) bands were emitted (Brewster 1834). At the time, the phenomenon of light absorption and emission was called opalescence or dispersive reflexion. In a lengthy paper, published 18 years later, in 1852, G.G. Stokes, the 13th Lucasian Professor of Mathematics at Cambridge University (Isaac Newton was the 2nd), wrote in discussing "dispersive reflexion" in a footnote, "I confess I do not like this term. I am almost inclined to coin a word, and call the appearance fluorescence, from fluor-spar, as the analogous term opalescence is derived from the name of a mineral" (Stokes 1852, p. 479). Thus, the term fluorescence came to be named after a mineral.

The physical phenomenon responsible for fluorescence would not be understood for more than half a century, until fundamental discoveries of quantum mechanics allowed for the concepts of excited states of electrons in elements and molecules. However, in 1931, a century after Brewster's observations, an Austrian scientist, Hans Kautsky, and his graduate student, A. Hirsch, working at the University of Heidelberg, reported that in living leaves, chlorophyll fluorescence changed over a period of seconds (for reviews, see Lichtenthaler 1992, Govindjee 1995). They observed the phenomenon with their naked eyes and wrote a one-page paper in *Naturwissenschaften* (Kautsky & Hirsch 1931). In the early phase of illumination, chlorophyll fluorescence rose, but after a few seconds, it declined and reached a steady state. The variability could be diminished by freezing or the addition of hydrogen cyanide.

Why is chlorophyll fluorescence in living cells variable? Surely, if it were variable in solvent extracts, this would have been reported much earlier. It would take more than 50 years to understand the causes of the variability. Indeed, in vivo chlorophyll fluorescence is the only natural biological process where the fluorescence yield varies on timescales of seconds or longer.

The discovery of two photosystems in oxygenic photosynthesis by Emerson (1957) led to a huge effort to understand how light could drive electron transfer reactions in life. By the early 1960s, it was realized that virtually all of the chlorophyll fluorescence in living cells emanated from photosystem II (PSII), which is the reaction center responsible for splitting water (Duysens et al. 1961, Duysens & Sweers 1963). From that point, variations in chlorophyll fluorescence in vivo were examined not simply in the context of excited states of chlorophyll molecules, but rather in the context of how various biological electron donors and acceptors could modify fluorescence.

In 1972, David Mauzerall, using a pump-and-probe laser technique, showed that the initial rise in chlorophyll fluorescence in living *Chlorella* cells was in the microsecond time domain, far too slow to be attributed to primary processes (i.e., direct photobiological electron transfer reactions, which are in the picosecond time domain) (Mauzerall 1972). Hence, there had to be secondary processes that modified chlorophyll fluorescence yields over time. Here, it is important to understand what a chlorophyll fluorescence yield means. The quantum yield of fluorescence is defined as the ratio of the photons reradiated to those absorbed. It is not an easy measurement to make. How many photons are actually absorbed by the fluorescent molecules? It took another decade to understand that the chlorophyll fluorescence yield was modified by biochemical processes in the reaction center of PSII.

The concept that chlorophyll fluorescence yields could be biochemically modified was first proposed by the Dutch biophysicist Louis Duysens (1956). The details have been described in many papers (see Papageorgiou & Govindjee 2004), but the crux of the matter is that the biochemists and biophysicists discovered a series of electron transfer reactions in PSII that modified fluorescence yields. The primary processes responsible for the change in fluorescence are the photooxidation of a specific chlorophyll molecule, P680, called a donor, and the reduction of one

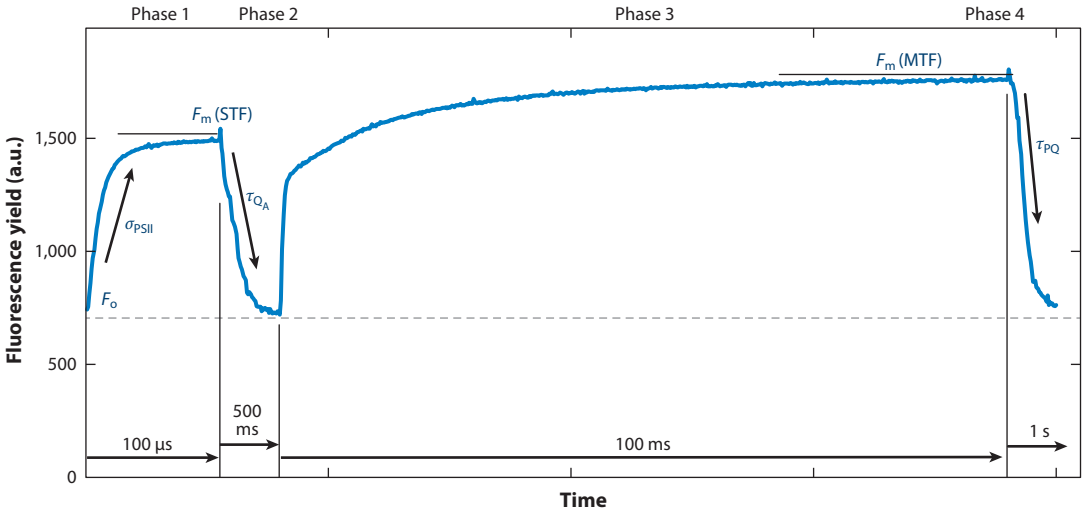

Figure 1

An example of the kinetics of fluorescence yields recorded with microsecond time resolution. There are four phases. In the first phase (100 µs), a strong short flash, called a single turnover flash (STF), is applied to cumulatively saturate photosystem II (PSII) and measure the fluorescence induction from F_o to F_m. The rate of the rise is related to the functional absorption cross section of PSII. The second phase (500 ms), obtained by weak modulated light, is used to measure the relaxation kinetics of fluorescence yield on micro- and millisecond timescales. This is related to the oxidation of the primary acceptor, Q_A. The third phase, obtained by a strong long pulse of 100-ms duration, called a multiple turnover flash (MTF), is applied to saturate PSII and the plastoquinone pool. The fourth phase (1 s) is observed when weak modulated light is applied to measure the kinetics of the electron transport between PSII and PSI, i.e., reoxidation of plastoquinol. Note that the time axis is linear for induction phases and logarithmic for relaxation phases.

or more acceptors. The primary acceptor in PSII is a protein-bound plastoquinone, designated Q_A (Q is short for quencher, and was named by Duysens). The changes in the fluorescence yields of chlorophyll, originally observed by Kautsky & Hirsch (1931), were subsequently understood to be a photobiological reaction resulting in the oxidation of a bound chlorophyll molecule within the reaction center designated P680 and the subsequent reduction of Q_A (see the section titled Photochemical Processes in Photosystem II on the Timescale of a Single Photochemical Turnover). This reaction, described by Mauzerall, occurs on timescales of 100 µs or less (see **Figure 1**).

It should be noted that chlorophyll *a* has two major absorption bands: One is a broad band centered in the blue portion of the spectrum around 440 nm, called the Soret band, and the second is centered in the red portion around 675 nm in vivo, called the Q_y band (a spectroscopic term, not to be confused with a quencher). Light absorbed in the Soret band is transferred within the molecule to the lower-energy bands on timescales of 10^{-15} s. All chlorophyll fluorescence emanates from the Q_y band. In optically thin solutions of phytoplankton (which is virtually every case in the oceans), chlorophyll emission is centered at around 685 nm. The small (~10 nm) shift from the absorption band to the emission band is called the Stokes shift—named after the same G.G. Stokes who coined the word fluorescence. Note that in optically opaque samples, such as in higher-plant leaves, chlorophyll fluorescence is emitted at even longer wavelengths, with the peak at approximately 715–730 nm, because the photons emitted at 685 nm are reabsorbed before they are radiated to the environment. Hence, application of terrestrial plant fluorometers to aquatic systems results in extremely low sensitivity.

In 1972, Warren Butler, a biophysicist, using Mauzerall's data, suggested the basic model of the redox coupling between the donor/acceptor pair as the source of variable fluorescence

Table 1 Variable fluorescence notations and terminology

Term	Description
PSII	Photosystem II
ETR	Electron transport rate
NPQ	Nonphotochemical quenching
σ_{PSII}^{opt}	Optical absorption cross section of PSII ($Å^2$)
σ_{PSII}	Functional absorption cross section of PSII ($Å^2$)
F_o, F_m	Minimum and maximum yields, respectively, of chlorophyll *a* fluorescence measured in a dark-adapted state (arbitrary units)
F_v	Variable fluorescence ($=F_m - F_o$)
F_v/F_m	Maximum quantum yield of photochemistry in PSII, measured in a dark-adapted state (dimensionless)
p	Connectivity factor, defining the probability of the exciton energy transfer between individual photosynthetic units (dimensionless)
F'_o, F', F'_m	Minimum, steady-state, and maximum yields, respectively, of chlorophyll *a* fluorescence measured under ambient light (arbitrary units). F'_o can be measured after a brief (~1 s) period of darkness to promote the opening of all reaction centers. Here, F'_o and F'_m correspond to fully open and fully closed reaction centers, respectively. The prime character indicates that the measurements are made under ambient light.
$\Delta F'$	Change in the fluorescence yield measured under ambient light ($= F'_m - F'$), called in some literature F'_q
$\Delta F'/F'_m$	Quantum yield of photochemistry in PSII, measured under ambient light [$\Phi_{PSII} = (F'_m - F') / F'_m$] (dimensionless). In some literature, this parameter is given as F'_q/F'_m.
F'_v/F'_m	Quantum efficiency of photochemistry in open reaction centers of PSII, measured in a light-adapted state [$= (F'_m - F'_o) / F'_m$] (dimensionless)
n_{PSII}	Ratio of PSII to the number of chlorophyll *a* molecules in the cell. This ratio is called the size of the PSII unit.
PQ	Photosynthetic quotient, which is the ratio of O_2/CO_2 evolved/fixed in the process of photosynthesis
$\phi_{e,C}$	Electron requirement for carbon fixation (the number of electrons required to fix one CO_2) [$= (1 / k\ PQ)^{-1}$]
$1/\tau$	Photosynthetic turnover rate
k_P, k_F, k_T	Rates of three possible pathways of energy use and dissipation in photosynthesis: photochemistry, fluorescence, and heat, respectively

(Butler 1972, 1978). In retrospect, the idea is both simple and original. Furthermore, Butler realized that photons absorbed by a photosynthetic organism had three fates: They could be photochemically used to make a biological reductant, they could be emitted to the environment as fluorescence, or they could generate heat (which obviously was not biologically useful). Butler reasoned that the sum of the quantum yields (ϕ) of each pathway had to be 1.00:

$$\phi_P + \phi_F + \phi_T = 1.00. \quad 1.$$

Hence, if one could measure the quantum yield of two of the three pathways, the third could be easily calculated.

Butler further realized that the quantum yield of photochemistry was dependent on the rate constants of the three possible pathways; photochemistry, fluorescence, and heat (with the rates k_P, k_F, and k_T, respectively; **Table 1**). What does the change in variable fluorescence mean? In the dark, when all the electron donors are reduced and the acceptors are oxidized, the quantum yield of fluorescence is minimal and is designated F_o. In a saturating flash, all the primary electron acceptors become reduced and fluorescence rises to a maximum; that value is designated F_m. It should be noted that fluorescence yields in this context have arbitrary units—that is, they are relative. The difference between F_m and F_o is called variable fluorescence, designated F_v.

When measuring the fluorescence yield of photosynthetic organisms in the dark, we can see that

$$\phi_{F_o} = \frac{k_F}{k_P + k_F + k_T}. \quad 2.$$

Here, the fluorescence yield is minimal (F_o), while the photochemistry is maximal. However, once a saturating light pulse is used such that all reaction centers are closed (i.e., all electron donors in PSII are oxidized, and all primary electron acceptors are reduced), k_P diminishes to zero, and the fluorescence yield rises to a maximum (F_m):

$$\phi_{F_m} = \frac{k_F}{k_F + k_T}. \quad 3.$$

Normalizing the variable fluorescence to the maximal fluorescence, we obtain the quantum yield of PSII photochemistry, ϕ_{PSII}:

$$\phi_{PSII} = \frac{k_P}{k_P + k_F + k_T} = \frac{F_v}{F_m}. \quad 4.$$

Hence, one of the parameters that determines the quantum yield of photosynthesis in Equation 1 could be solved from variations in the fluorescence of chlorophyll *a* in vivo.

In a dark-adapted state or under low irradiance (when k_t is constant), the quantum yield of chlorophyll fluorescence, ϕ_F, is inversely related to the quantum yield of photochemistry in PSII, $\phi_{PSII} = F_v/F_m$:

$$\phi_F = \phi_{F_m}(1 - F_v/F_m). \quad 5.$$

This biophysical model predicts an inverse linear relationship between the quantum yield of photochemistry and that of chlorophyll fluorescence. However, by the early 1980s it was realized that exposure to high irradiance can generate a suite of thermal dissipation mechanisms, collectively called nonphotochemical quenching (NPQ). This photoprotective response markedly decreases the quantum yield of chlorophyll fluorescence at high background light. Hence, the relationship between fluorescence yield and photochemistry becomes highly nonlinear as NPQ phenomena play an increasingly large role in energy dissipation (Falkowski et al. 2017).

FUNCTIONAL ABSORPTION CROSS SECTION OF PHOTOCHEMISTRY

If it takes approximately 100 μs for fluorescence to rise from F_o to F_m during a saturating single turnover flash (**Figure 1**), what controls the rate of the rise? The sequential reduction of the primary acceptor in PSII requires that each electron transferred from the primary donor be driven by the absorption of a single quantum (this is one of Einstein's rules). The rise of fluorescence during a saturating single turnover flash is driven by a transition of reaction centers to the closed state, and the rate of this rise can be displayed in a time-independent manner:

$$dC/dt = -\sigma I, \quad 6.$$

where C is the fraction of open reaction centers, σ is the functional (sometimes called the effective) absorption cross section of the process (in units of $Å^2$ quanta^{-1} or m^2 quanta^{-1}), and I is the photon flux density of the excitation light. The resulting fluorescence rise obeys a cumulative one-hit Poisson distribution, where the normalized fluorescence yield is

$$F_v(t)/F_v^{max} = 1 - \exp(-\sigma I t). \quad 7.$$

The product σI describes the efficiency with which light is absorbed by a reaction center that drives photochemistry—in this case, PSII. This absorption cross section is a measure of the probability that an absorbed photon will drive a photochemical reaction (Ley & Mauzerall 1982, Mauzerall 1986). It should be noted that the functional cross section is not the physical size of the antenna complexes of PSII; it is related to the quantum efficiency by which the antenna complexes harvest light and transfer the excitation energy to a reaction center. It should also be noted that the functional absorption cross section is wavelength dependent.

The functional absorption cross section of PSII is critical to deriving absolute photosynthetic electron transport rates (ETRs) in algal cells (see the section titled Modeling Electron Transport Rates from Variable Fluorescence). The cumulative one-hit Poisson distribution predicts that fluorescence yield follows an exponential rise. In a more general case, when the reaction centers share excitation energy among the light-harvesting pigment–protein complexes, the fluorescence rise becomes sigmoidal and can be accurately described by incorporating a connectivity parameter, p, that defines the probability of transfer of excitons between reaction centers (Paillotin 1976, Ley & Mauzerall 1986, Kolber et al. 1998, Joliot & Joliot 2003).

PHOTOCHEMICAL PROCESSES IN PHOTOSYSTEM II ON THE TIMESCALE OF A SINGLE PHOTOCHEMICAL TURNOVER

What does the term saturating single turnover flash mean? In the simple model of variable fluorescence and its relation to the quantum yield of photochemistry in PSII presented above, there is an implicit assumption that there is a single electron acceptor. The primary electron acceptor is indeed a single molecule: a plastoquinone bound to a protein within the PSII reaction center complex. This quinone, called Q_A (the quencher) accepts and stabilizes one electron per photon absorbed within the reaction center. Indeed, this is the molecule that is reduced within several hundred picoseconds after photon absorption and stores the electron for ~100 μs before it is transferred further down the electron transport chain. If, however, saturating light is continuously shone on the sample, the fluorescence will rise to a higher level (**Figure 1**). This phenomenon is due to the transfer of the electrons from Q_A to a second plastoquinone molecule, Q_B, which is mobile. Ultimately, Q_B will accept two electrons and subsequently bind two protons, and then leave its binding site to ferry the electrons down the photosynthetic electron transport chain (Bowes & Crofts 1980, Crofts & Wright 1983). Note that in this process, the electrons and protons come from the photochemical splitting of water, but molecular hydrogen (H_2) is never physically formed. The hydrogen atoms are further split into protons and electrons. The protons carried by Q_B will be dumped into membrane pockets of the chloroplast, leading, in the steady state, to a transmembrane pH gradient of approximately 3 units—i.e., 1,000-fold more protons on one side of the membrane than the other. The change in pH results in an electrical field across the membrane that affects the electronic dipole of membrane-bound pigments in the light-harvesting antenna complexes, including chlorophyll *a*, and is critical to the formation of ATP via chemosis (Mitchell 1977). The resulting charge gradient across the thylakoid membrane (called the Stark effect, or sometimes the electrochromic shift) leads to an increase in the quantum yield of fluorescence on timescales longer than 100 μs, when a multiple turnover flash is applied (Bailleul et al. 2010). This level of fluorescence does not truly reflect primary charge separation, yet it is often reported in the literature (especially older literature) because most measurements of variable fluorescence are too slow to record the initial rise.

Why do multiple turnover flashes overestimate F_v/F_m? Such saturating flashes can result not only in the reduction of Q_A but also in the reduction of plastoquinone to plastoquinol. Plastoquinone, but not plastoquinol, is a quencher of chlorophyll fluorescence (Vernotte et al. 1979,

Kramer et al. 1995). As a result, when F_o is measured prior to a multiple turnover flash, when the plastoquinol pool is oxidized, and F_m is measured at the end of such a flash, when the plastoquinone pool is reduced, the resulting F_v/F_m is overestimated by as much as ~20%, making the quantitative interpretation of multiple turnover–based fluorescence measurements ambiguous.

PHOTOSYNTHETIC TURNOVER RATES

The photosynthetic turnover time (τ) is defined as the time required for the products of primary photochemical reactions (i.e., electrons produced as a result of charge separation in reaction centers) to complete the whole cycle of transfer from reaction centers to ribulose-1,5-bisphosphate carboxylase/oxygenase (RuBisCO) and CO_2 fixation (Herron & Mauzerall 1971, Myers & Graham 1971). The reciprocal of the turnover time ($1/\tau$) is the turnover rate, which determines the maximum rate of this process (P^{max}).

Measurements of photosynthetic turnover rates are fundamentally important for understanding the variability of primary production in the ocean, as these rates determine P^{max}. In turn, P^{max} is the key variable that determines the water column integrated primary production in the global ocean (Behrenfeld & Falkowski 1997).

NONPHOTOCHEMICAL QUENCHING

Curiously, one protein in the core of the reaction center of PSII, called D1, is degraded by reactive oxygen species approximately every 30 min in natural light (Campbell & Tyystjärvi 2012). This degradation leads to a reduction in photosynthetic carbon fixation in high light, a phenomenon called photoinhibition (Long et al. 1994). To minimize the damage, plants, eukaryotic algae, and many cyanobacteria have evolved several photoprotective mechanisms that are activated under high-light conditions.

On a timescale of minutes, photoprotective mechanisms enhance the thermal dissipation of absorbed energy to prevent oxidative damage to the D1 protein. These photoprotective processes are called NPQ (see Demmig-Adams et al. 2014). Although the molecular and biochemical mechanisms of NPQ differ among phytoplankton taxa, the result is the same: NPQ processes lead to a competing energy dissipation pathway within the antenna that simultaneously reduces the flux of absorbed energy used for photochemistry. The biophysical phenomenon is manifested in a reduction in the functional absorption cross section of the reaction centers that is reversible on timescales of seconds to minutes (Gorbunov et al. 2011, Kuzminov & Gorbunov 2016, Buck et al. 2019).

Historically, the phenomenon that chlorophyll fluorescence is quenched by high light was discovered in aquatic ecosystems long before it was called NPQ (e.g., Kiefer 1973, Abbott et al. 1982). What caused the quenching was not understood. Attempts to inhibit this process by the addition of 3-(3,4-dichlorophenyl)-1,1-dimethylurea (DMCU)—which blocks the reduction of the plastoquinone pool by irreversibly binding to the Q_B site in the PSII reaction center, thereby essentially locking the cells in the F_m state—had no effect, indicating that this quenching phenomenon was not due to photochemistry. Falkowski et al. (1986) and Schreiber et al. (1986) independently suggested that fluorescence quenching by high light was a result of carotenoids absorbing the excitation energy in the light-harvesting complexes and dissipating it as heat. The major component of NPQ, called energy- or pH-dependent quenching, is induced by the transmembrane ΔpH (Horton et al. 1996). The thylakoid lumen, having low pH, triggers deepoxidation of violaxanthin to zeaxanthin via an intermediate, antheraxanthin (Demmig-Adams & Adams 1996). This reversible reaction, called the xanthophyll cycle, is enzymatically catalyzed (Yamamoto 1979) and induces conformational changes in light-harvesting complex II that

significantly increase thermal dissipation in the antenna complexes (Ruban et al. 2007). Many species of Bacillariophyceae, Chloromonadophyceae, Chrysophyceae, Euglenophyceae, Xanthophyceae, and Dinophyceae exhibit a similar light-stimulated conversion of diadinoxanthin to diatoxanthin (Demers et al. 1991, Olaizola et al. 1994, Brown et al. 1999, Falkowski & Raven 2007). Because the NPQ phenomenon results in a highly nonlinear relationship between chlorophyll concentrations in vivo and fluorescence yields, it severely limits the ability to use in vivo chlorophyll fluorescence to quantify chlorophyll biomass in the world oceans (Falkowski & Kolber 1995).

Another NPQ mechanism is attributed to enhanced thermal dissipation in the PSII reaction centers themselves. Excess light may lead to an accumulation of oxidized PSII reaction centers (P680+) that capture excitons as efficiently as open centers do but then dissipate the exciton energy as heat (Schweitzer & Brudvig 1997). Furthermore, photoinhibition by supraoptimal light results in degradation of the PSII reaction center protein D1 but enhances thermal dissipation in PSII centers (Long et al. 1994). Finally, irradiance-induced phosphorylation of light-harvesting complexes can induce migration of a fraction of the antenna complexes from PSII to PSI, thereby diverting a portion of excitation flux away from PSII (the so-called state-1-to-state-2 transitions) (Campbell et al. 1998).

Cyanobacteria and eukaryotes have similar structures of the photosystems and the electron transport chain but differ in the way the light-harvesting systems are organized. Most (but not all) cyanobacteria utilize large, water-soluble light-harvesting complexes called phycobilisomes, which are bound to the surface of the thylakoid membrane (Sidler 1994, MacColl 1998, Ke 2001). While in plants and eukaryotic algae the NPQ mechanisms act to dissipate excess energy directly from chlorophyll *a*, in cyanobacteria they lead to a competing energy dissipation pathway in phycobilisomes (El-Bissati et al. 2000, Wilson et al. 2006). An orange carotenoid protein (OCP) has been implicated as a blue-green light sensor that triggers and induces NPQ in cyanobacteria (Wilson et al. 2007, Kirilovsky & Kerfeld 2016). The presence (or absence) of the NPQ mechanism in prokaryotic algae is determined by the presence (or absence) of the OCP-encoding gene (Kirilovsky & Kerfeld 2016). For example, the whole genome of *Prochlorococcus* sp., which is the most abundant species in tropical oceans, revealed the lack of the OCP gene. As a result, *Prochlorococcus* does not appear to exhibit the NPQ mechanism. Fluorescence quenching observed in natural *Prochlorococcus* communities under strong irradiance at noon is due to thermal dissipation in photoinhibitory damaged PSII reaction centers, which is not true of NPQ.

NPQ is classically defined as the increase in thermal dissipation induced by excess light, which, by inference, results in quenching of F_m fluorescence. To a first approximation, NPQ is zero in dark-adapted cells and increases with ambient irradiance. In some literature, NPQ is considered the total thermal dissipation, which obviously causes confusion with NPQ data interpretation. Several parameters have been used elsewhere to quantify NPQ. A commonly used NPQ parameter is defined as follows (Bilger & Bjorkman 1990):

$$\mathrm{NPQ} = (F_m - F'_m)/F'_m. \quad 8.$$

The quantum yield of NPQ—that is, the fraction of absorbed photons that is thermally dissipated via NPQ—can be calculated as follows (Gorbunov et al. 2001):

$$\phi_{\mathrm{NPQ}} = (F_m - F'_m)/F_m. \quad 9.$$

This calculation is analogous to that used to derive the quantum yield of photochemistry (F_v/F_m) from variable fluorescence. When a fraction of reaction centers are dynamically open under a given level of ambient light and photochemical quenching by these open centers competes with and reduces the NPQ yield, the resulting quantum yield of NPQ can be estimated as (Hendrickson

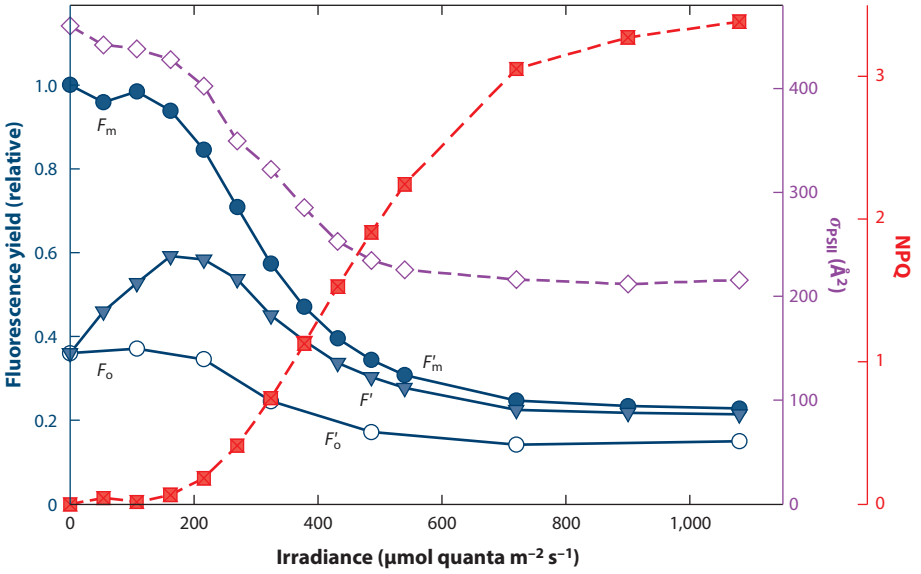

Figure 2

The irradiance dependence of the quantum yields of chlorophyll fluorescence in a marine diatom, *Phaeodactylum tricornutum*. F_o and F_m are the minimum (open reaction centers) and maximum (closed centers) yields, respectively, measured in dark-adapted cells. F'_o and F'_m are the minimum (fully open centers) and maximum (closed centers) fluorescence yields, respectively, measured in a light-adapted state. F' is the actual quantum yield measured under ambient light. The irradiance dependence of F' corresponds to that of the quantum yield of solar-induced fluorescence recorded remotely from a satellite platform. The magnitude of nonphotochemical quenching (NPQ) is calculated from the light-induced decrease in the maximum fluorescence yield and is characterized by the NPQ parameter, $\mathrm{NPQ} = (F_m - F'_m) / F'_m$. Measurements of variable fluorescence as a function of irradiance are the first step in reconstruction of the irradiance dependence of photosynthetic electron transport rates and the fluorescence-based rates of primary production.

et al. 2004, Kramer et al. 2004)

$$Y(\mathrm{NPQ}) = F'/F'_m - F'/F_m. \qquad 10.$$

The Y(NPQ) parameter is affected by the fraction of open reaction centers and, in essence, reflects the mixture of NPQ and photochemical quenching. When the fraction of dynamically open centers decreases to zero under saturating ambient light, F' approaches F'_m (**Figure 2**), and Y(NPQ) is equal to ϕ_{NPQ}.

It should be noted that NPQ leads to a diel cycle in fluorescence yields in the upper ocean, where chlorophyll fluorescence (e.g., F' or F'_m) is lowest at midday and highest at night (**Figure 3**). The diel variations in chlorophyll fluorescence are driven by NPQ processes induced by solar light; therefore, the NPQ capacity is affected by the species composition and physiological status of phytoplankton, such as nutrient limitation (Gorbunov & Chekalyuk 1992, Schuback et al. 2017, Schallenberg et al. 2020). As a result, the magnitude of midday fluorescence quenching is usually higher in nutrient-limited phytoplankton communities (Gorbunov & Chekalyuk 1992) (**Figure 3**). This phenomenon is critical in the interpretation of the solar-induced fluorescence of chlorophyll from satellites (see the section titled Phytoplankton Physiology from Space: Validation and Calibration of Solar-Induced Chlorophyll Fluorescence Yields).

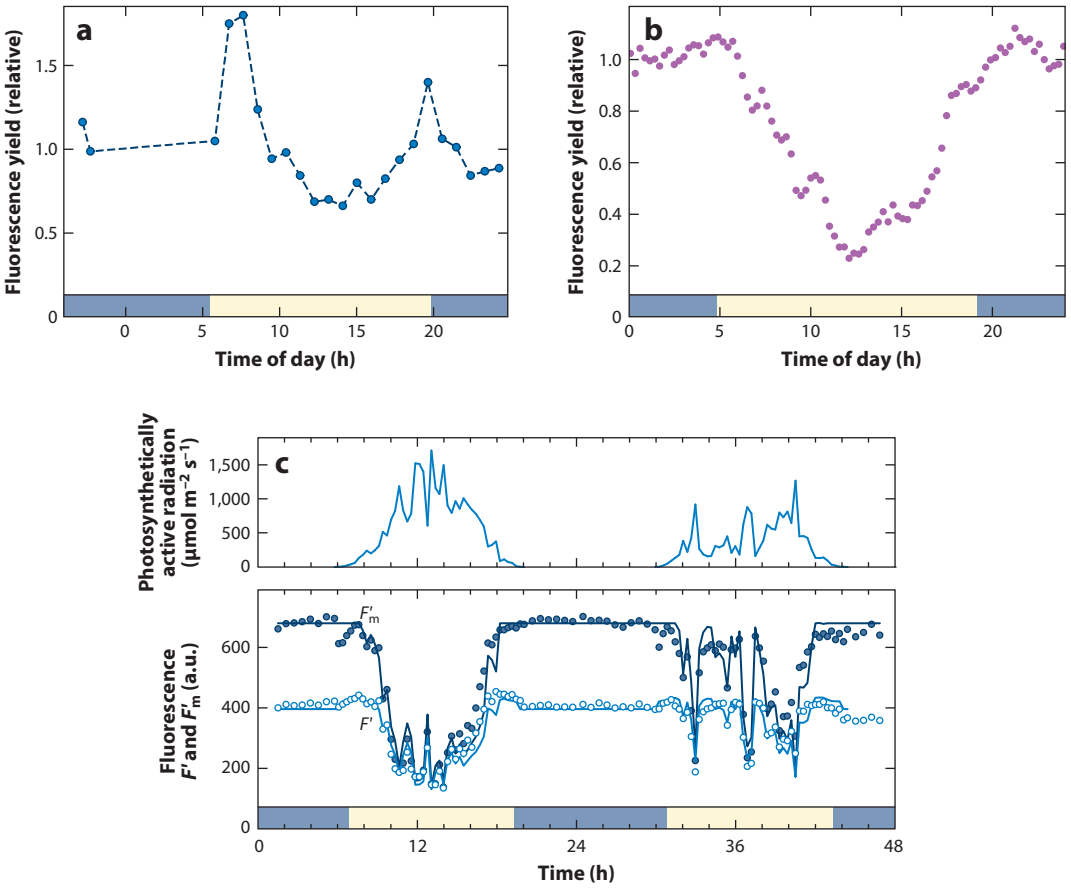

Figure 3

Diel variations of in situ chlorophyll fluorescence yields: (*a*) a nutrient-replete phytoplankton community in a coastal region in the Mediterranean Sea, (*b*) an iron-stressed phytoplankton in the Southern Ocean, and (*c*) the symbiotic coral *Orbicella faveolata* on a shallow coral reef. Fluorescence yields F' in panel *a* were recorded in situ in the near-surface layer by a pump-and-probe lidar system (Gorbunov & Chekalyuk 1992), fluorescence yields F' in panel *b* were recorded using a fluorescence induction and relaxation (FIRe) system in near-surface phytoplankton exposed and adapted to in situ irradiances (data are from Lin et al. 2016), and fluorescence yields in panel *c* at F' and F'_m levels were recorded by a moored fast repetition rate (FRR) fluorometer (Gorbunov et al. 2001). The influence of nonphotochemical quenching (NPQ) upon fluorescence is highly dynamic and adjusts to irradiance changes on timescales consistent with the passage of clouds across the sky (panel *c*). Note the striking difference in the magnitude of diel variations between nutrient-replete (panel *a*) and nutrient-limited (panel *b*) phytoplankton as the NPQ capacity increases in the nutrient-stressed phytoplankton.

THE USE OF VARIABLE FLUORESCENCE TO INFER PHYTOPLANKTON PHOTOPHYSIOLOGY AND PHOTOSYNTHETIC RATES IN AQUATIC ECOSYSTEMS

Since the mid-1980s, it has been realized that variable fluorescence could be used to understand the photophysiology of marine photoautotrophs. Indeed, variable chlorophyll fluorescence is the most sensitive, nondestructive signal detectable in the upper ocean that reflects instantaneous phytoplankton photophysiology (Kolber & Falkowski 1993, Kolber et al. 1998). Variable chlorophyll fluorescence techniques are increasingly used to estimate the biomass and physiological status

of phytoplankton and benthic organisms in marine ecosystems (for a review, see Falkowski et al. 2004).

Although variable fluorescence signals in marine sciences were originally measured using pump-and-probe techniques, such an approach is extremely tedious (Kolber & Falkowski 1993). The development of high-intensity light-emitting diodes, highly sensitive photodetectors, and fast computers allowed for the invention of novel approaches and instrumentation. These include fast repetition rate (FRR) fluorometry (Kolber et al. 1998; Gorbunov et al. 1999, 2000, 2001) and its technological successors, such as the fluorescence induction and relaxation (FIRe) technique (Gorbunov & Falkowski 2005, 2021; Gorbunov et al. 2020). These optical measurements are sensitive, fast, and nondestructive and can be done in real time and in situ in the world's oceans.

Measurement of FIRe fluorescence parameters over a range of ambient irradiances (**Figure 2**) permits one to reconstruct the light-driven electron flux in PSII, commonly called the photosynthetic ETR. ETR is a function of irradiance and is calculated from measurements of variable fluorescence over a range of photosynthetically active radiation levels (Kolber & Falkowski 1993). ETR is proportional to the product of irradiance and the quantum yield of photochemistry in PSII measured under ambient light. Analysis of these photosynthesis-versus-irradiance curves provides the maximum rate of photosynthetic electron transport (ETR_{max}) and the light-saturation parameter (E_k). The latter is the intercept of the initial slope and the maximum rate of a photosynthesis-versus-irradiance curve and is the only point in this curve where light harvesting is balanced by electron transport (Falkowski & Raven 2007).

RATIONALE FOR USING VARIABLE FLUORESCENCE TO DERIVE INSTANTANEOUS RATES OF PRIMARY PRODUCTION

Measurement of absolute ETR per PSII unit is the starting point in retrieving the photosynthetic rates and rates of primary production. One measure of primary production is the chlorophyll-specific rate of CO_2 assimilation (i.e., CO_2 fixed per unit chlorophyll *a*, often called the assimilation number in marine sciences),

$$P^{\mathrm{chl}} = \mathrm{ETR} n_{\mathrm{PSII}} 0.25/\mathrm{PQ}, \qquad 11.$$

where n_{PSII} is the ratio of PSII to chlorophyll *a* molecules, 0.25 is the quantum yield of O_2 evolution (i.e., four electrons are needed to evolve one O_2), and PQ is the ratio O_2/CO_2, called the photosynthetic quotient.

The n_{PSII} value cannot be measured directly using variable fluorescence alone (Kolber & Falkowski 1993). Because n_{PSII} is, at a first approximation, proportional to the physical size of the PSII unit, it can be estimated from the optical absorption cross section of PSII or the functional absorption cross section of PSII (σ_{PSII}), assuming that the functional cross section is proportional to the optical one (Oxborough et al. 2012). However, variations in the pigment packaging effect (Falkowski et al. 1985) and the ratio of chlorophyll *a* to accessory pigments introduce errors to the relationship between n_{PSII} and σ_{PSII}. Although n_{PSII} may range from 0.001 to 0.007 reaction centers per chlorophyll *a* molecule among algal species, the FRR model assumes $n_{\mathrm{PSII}} = 0.002$ reaction centers per chlorophyll *a* molecule, a typical average value for eukaryotic algae (Kolber & Falkowski 1993). Because mesoscale variations in σ_{PSII} in the ocean are relatively small, as compared with the above range of laboratory values of n_{PSII} (0.001–0.007 reaction centers per chlorophyll *a* molecule), uncertainties in n_{PSII} appear to be a minor source of errors of variable fluorescence estimates of primary production in the ocean. Equation 11 can also be rewritten as

$$P^{\mathrm{chl}} = \mathrm{ETR} n_{\mathrm{PSII}} (\phi_{\mathrm{e,C}})^{-1}. \qquad 12.$$

Here, $\phi_{e,C}$ is the electron requirement for carbon fixation, which is defined as the number of electrons produced in PSII photochemistry required to accumulate one cellular carbon atom (Kolber & Falkowski 1993, Lawrenz et al. 2013).

The bulk rate of CO_2 fixation is calculated by multiplying Equation 11 by the chlorophyll *a* concentration, [Chl-a]:

$$P^{CO_2} = \mathrm{ETR}\, n_{PSII} 0.25/\mathrm{PQ}\, [\text{Chl-a}]. \quad 13.$$

The chlorophyll *a* concentration can be deduced from FRR/FIRe measurements of F_m fluorescence yields calibrated against standard measurements of chlorophyll *a* concentration in solvent extracts.

PQ and $\phi_{e,C}$ cannot be measured directly using fluorescence techniques and may vary with nutrient stress. Uncertainties in $\phi_{e,C}$ are the main source of errors in fluorescence-based estimates of primary production. For nutrient-replete conditions and a moderate degree of nitrogen stress, PQ is approximately 1.4, and this number increases with severe nitrogen limitation (Laws 1991, Lawrenz et al. 2013). Comparisons of amplitude-based variable fluorescence and ^{14}C measurements of primary production in diverse biogeochemical regions of the ocean revealed that the electron requirements (and electron yields) for carbon fixation are influenced by the extent of nutrient limitation and also may vary with taxonomy and other factors (Kromkamp et al. 2008, Lawrenz et al. 2013, Zhu et al. 2017, Hughes et al. 2018b). Closer examination of environmental factors that may control the electron requirements suggests that nutrients—specifically nitrogen limitation—is critical (Hughes et al. 2018b, Ko et al. 2019, Gorbunov & Falkowski 2021). The electron yield for net primary production, Φ_{NPc}, or the ratio of the number of accumulated cellular carbon atoms to the number of electrons produced by photochemistry in PSII, is maximal under nitrogen-replete conditions and decreases down to near zero under severe nitrogen starvation (Gorbunov & Falkowski 2021). The application of fluorescence kinetic analysis offers a simple fluorescence-based indicator to predict the electron yields of carbon fixation under nitrogen limitation (**Figure 4**).

MODELING ELECTRON TRANSPORT RATES FROM VARIABLE FLUORESCENCE

Modeling ETRs from variable fluorescence is critical to determine the fate of absorbed photons in photosynthetic processes. There are two main approaches to model ETRs from variable fluorescence: amplitude based and kinetic (Gorbunov & Falkowski 2021). Below, we describe and discuss these two basic methods.

Amplitude-Based Fluorescence Measurements of Electron Transport Rates

The absolute ETR per open PSII reaction center is calculated from the product of light intensity (*E*), the optical absorption cross section of PSII (i.e., how much light is absorbed by a PSII unit), and the quantum yield of photochemistry in PSII, Φ_{PSII} (i.e., the portion of absorbed photons that produce electron flow in PSII). This product must be further multiplied by a fraction of dynamically open centers to reflect the fact that a fraction of reaction centers become dynamically closed under ambient light and only the remaining open centers contribute to photosynthetic energy utilization. The fraction of open reaction centers (also called the coefficient of photochemical quenching) can be measured by the variable fluorescence technique as a ratio of variable fluorescence under a given irradiance ($\Delta F'$) to the maximum variable fluorescence (F_v') for this irradiance level. F_v' can be measured after a brief (~1 s) period of darkness to promote the opening of all

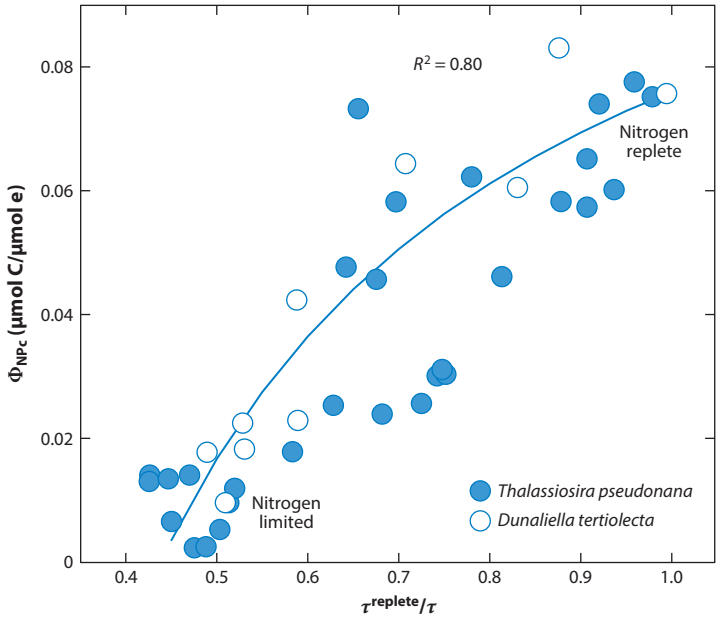

Figure 4

Effect of nitrogen limitation on the electron yield of net primary production (Φ_{NPc}), in relation to photosynthetic turnover rates ($1/\tau$). The plot combines data for two model phytoplankton species: the diatom *Thalassiosira pseudonana* and the green alga *Dunaliella tertiolecta*. The turnover rates were calculated from the analysis of fluorescence induction and relaxation (FIRe) relaxation kinetics under saturating irradiance. τ and $\tau^{replete}$ are the turnover times recorded in nitrogen-limited and nitrogen-replete samples, respectively. The $\tau^{replete}/\tau$ ratio characterizes the relative decrease in photosynthetic turnover rates under nitrogen limitation. Figure adapted from Gorbunov & Falkowski (2021).

reaction centers that were closed by ambient light. Therefore, ETR as a function of irradiance is expressed as follows:

$$\mathrm{ETR} = E\sigma_{\mathrm{PSII}}{}^{\mathrm{opt}}\Phi_{\mathrm{PSII}}(\Delta F'/F'_{\mathrm{v}}). \qquad 14.$$

The product of the optical absorption cross section and the quantum yield of photochemistry in PSII is defined as the functional absorption cross section of PSII ($\sigma_{\mathrm{PSII}} = \sigma_{\mathrm{PSII}}{}^{\mathrm{opt}}\ \Phi_{\mathrm{PSII}}$), and this parameter is directly measured using the FRR/FIRe technique. Therefore, Equation 14 can be modified as follows (Gorbunov et al. 2000, 2001):

$$\mathrm{ETR} = E\sigma'_{\mathrm{PSII}}(\Delta F'/F'_{\mathrm{v}}). \qquad 15.$$

Here, σ'_{PSII} is the functional absorption cross section of PSII, and $\Delta F'/F'_{\mathrm{v}}$ is the coefficient of photochemical quenching, recorded at a given level of ambient irradiance (E). $\Delta F'/F'_{\mathrm{v}}$ is the fraction of dynamically open reaction centers at a given level of irradiance. By definition, $\Delta F'/F'_{\mathrm{v}} = 1$ in the dark and decreases with irradiance as more reaction centers become dynamically closed by ambient light. The prime character indicates that the measurements are under ambient irradiance (E). Both σ'_{PSII} and $\Delta F'/F'_{\mathrm{v}}$ are a function of irradiance.

Measurement of σ_{PSII} is fundamental to infer the absolute ETR per PSII, which, by definition, is a concentration-independent parameter and reflects the physiological status of the cell, such as photoacclimation and nutrient limitation. For instance, measurements of absolute ETR per PSII offer a quantitative proxy for assessment of nitrogen limitation (Gorbunov & Falkowski 2021).

When NPQ is caused by thermal dissipation in the light-harvesting antennae, Equation 15 can be reduced to the following (Gorbunov et al. 2001):

$$\mathrm{ETR} = E\sigma_{\mathrm{PSII}}[(\Delta F'/F'_{\mathrm{m}})/(F_{\mathrm{v}}/F_{\mathrm{m}})], \qquad 16.$$

where $\Delta F'/F'_{\mathrm{m}}$ (sometimes denoted $F'_{\mathrm{q}}/F'_{\mathrm{m}}$ in recent literature) is the actual quantum yield of photochemistry in PSII at a given irradiance level. Note that $\Delta F'/F'_{\mathrm{m}}$ is the only irradiance-dependent variable in Equation 16 and that this parameter is directly measured by FRR/FIRe techniques. Use of Equation 15 requires measurements both under ambient light and after a brief period of darkness (e.g., in both open and dark chambers of the in situ FRR fluorometer). For instance, $F'_{\mathrm{v}} = F'_{\mathrm{m}} - F'_{\mathrm{o}}$ can be recorded only after a brief (~1 s) period of darkness, which is required for all reaction centers to open and for the fluorescence yield to reach the F'_{o} level. By contrast, Equation 16 includes parameters recorded only under ambient light, thus eliminating the need to make measurements in darkness.

Kinetic Fluorescence Measurements of Electron Transport Rates

Kinetic measurements of the absolute ETR rely on the rate of photosynthetic turnover ($1/\tau$), which defines the maximum ETR achieved under saturating irradiance, E_{max} (Gorbunov & Falkowski 2021). The shape of ETR(E) in relative units is reconstructed from the dependence of the quantum yield of photochemistry in PSII ($\Delta F'/F'_{\mathrm{m}}$ as a function of E):

$$\mathrm{ETR}_{\tau} = 1/\tau(E\Delta F'/F'_{\mathrm{m}})/[E_{\mathrm{max}}\Delta F'/F'_{\mathrm{m}}(E_{\mathrm{max}})]. \qquad 17.$$

Here, the relative ETR(E) = $E\ \Delta F'/F'_{\mathrm{m}}$ is normalized to unity by division to its maximum value $E_{\mathrm{max}}\ \Delta F'/F'_{\mathrm{m}}(E_{\mathrm{max}})$, which is recorded at saturating irradiance (E_{max}). Multiplication of the relative ETR by the photosynthetic turnover rate ($1/\tau$) provides the absolute ETR_{τ} per PSII unit. The value of $1/\tau$ is calculated directly from the FIRe-determined relaxation at saturating irradiance, using the kinetic analysis. The algorithm and operational protocol for kinetic measurements of ETR have been implemented in mini-FIRe instruments (Gorbunov & Falkowski 2021). The advantages and high accuracy of the kinetic measurements of ETRs have been documented by a strong correlation between these ETR measurements and growth rates (Gorbunov & Falkowski 2021).

Caveats and Limitations of Amplitude-Based Electron Transport Rate Measurements

Amplitude-based variable fluorescence techniques became a workhorse in plant physiology and oceanography to derive ETRs in phytoplankton and terrestrial plants (Genty et al. 1989, Kolber & Falkowski 1993, Hughes et al. 2018a). Obviously, these techniques do not measure ETR directly; instead, it is derived from biophysical models. Several models and modifications have been developed (Kolber & Falkowski 1993, Oxborough et al. 2012, Hughes et al. 2018a) to deduce ETR and rates of primary production in phytoplankton. All of these models rely on the use of multiple parameters, such as the quantum yield of photochemistry in PSII; the effective absorption cross section of PSII or absorption properties; the number of open and active reaction centers; and the spectral incident irradiance, including its penetration and attenuation within algal cells or leaves. As a consequence, errors in all parameters add up and inevitably increase the overall uncertainty of ETR calculations. Also, some of the model parameters, such as the absorption cross section and spectral irradiance, critically depend on the accuracy of instrument calibration. These caveats of amplitude-based ETR measurements can be alleviated by using an alternative fluorescence approach, namely kinetic analysis (Gorbunov & Falkowski 2021).

PHOTOPHYSIOLOGICAL EXPRESSION OF NUTRIENT STRESS

Oceanic primary production is fundamentally limited by the availability of nutrients, such as nitrogen and iron, and in some regions colimited by phosphorus. The paucity of nutrients in the global ocean leads to a substantial decrease in the efficiency of oceanic photosynthesis. On the global scale, oceanic phytoplankton operates at only ~50% of its potential maximum (Lin et al. 2016). At a first approximation, the distributions of nutrient stress in the global ocean show a meridional pattern, with most of the tropical and subtropical gyres being limited by the paucity of nitrogen, while polar and subpolar regions are limited by the paucity of iron (Moore et al. 2013). There are, however, marked exceptions to this rule. For example, although some areas in the North Atlantic show physiological signatures of iron stress in the summer (Nielsdottir et al. 2009, Ryan-Keogh et al. 2013), primary production in the North Atlantic is, in general, controlled by nitrogen availability. Photosynthesis in the Arctic ocean is controlled by nitrogen availability (Kulk et al. 2018, Mills et al. 2018, Lewis et al. 2019), and primary production in ice-free Arctic regions becomes severely nitrogen limited in the summer (Ko et al. 2020). On the other hand, vast high-nutrient, low-chlorophyll regions of the subarctic Pacific (Boyd et al. 1998) and eastern equatorial Pacific (Kolber et al. 1994; Behrenfeld et al. 1996, 2006; Behrenfeld & Kolber 1999), large regions of the South Pacific Gyre (Bonnet et al. 2008), and most of the Southern Ocean (Olson et al. 2000, Boyd & Abraham 2001, Boyd et al. 2001, Gervais et al. 2002, Coale et al. 2004) are limited by the paucity of iron (Boyd et al. 2007).

There are long-lasting debates in the oceanographic community about what the main control of primary production and phytoplankton growth in the global ocean is. Analysis of global distributions of primary production and nutrient concentration suggests that nitrogen limits primary productivity in most of the global ocean (Dugdale 1967, Eppley 1980, McElroy 1983). The development of robust, quantitative diagnostics of nutrient stress is crucial to improving our understanding of how nutrient availability affects phytoplankton growth rates and how it could be altered by climate change in the future.

The physiological effects of nutrient stress on phytoplankton growth are determined by the concentrations and fluxes of nutrients in the upper water column, and these fluxes are highly dynamic and variable in space and time. Also, susceptibility to nutrient stress varies significantly among phytoplankton species, taxa, and size groups (Sunda & Huntsman 1997, Litchman & Klausmeier 2008). Understanding and quantifying the effects of nutrient stress on primary production are fundamental tasks of biological oceanography, and addressing them requires the development of technologies for the quantitative analysis of nutrient stress in the ocean.

Measurements of a comprehensive suite of photosynthetic and physiological characteristics by variable fluorescence (**Table 2**) provide quantitative diagnostics of nutrient stress and its impact on growth rates (Falkowski et al. 2004, Gorbunov & Falkowski 2021). Assessment of the impact of nutrient limitation and other stressors on the physiology and growth of phytoplankton and terrestrial plants is traditionally based on measurements of the maximum quantum yield of photochemistry in PSII, or, simply put, the photosynthetic efficiency, known as the F_v/F_m ratio. Under nutrient-replete conditions (e.g., in coastal regions), F_v/F_m in natural phytoplankton

Table 2 Fluorescence diagnostics metrics of nutrient stress

Limiting factor	F_v/F_m	Fluorescence lifetime	t_{Q_A} in dark-adapted state	Photosynthetic turnover rate ($1/\tau$)
Iron	Significant decrease	Significant increase	Increase	No or little change
Nitrogen	Decrease or no change (under moderate nitrogen stress)	Increase or no change	No change	Decrease

populations is high, ranging from 0.55 to 0.65, when recorded using a single turnover flash (data from Lin et al. 2016 and many other field data). These values are very close to the maximum $F_v/F_m = 0.65$ typically observed in nutrient-replete algal cultures (Kolber et al. 1988, Kolber & Falkowski 1993), although some algal species exhibit inherently lower F_v/F_m (Suggett et al. 2009). Many environmental stressors lead to a decrease in F_v/F_m. In the case of nitrogen limitation, however, the relationship between F_v/F_m and phytoplankton growth rates is highly nonlinear (Kolber et al. 1988, Parkhill et al. 2001), which makes it impossible to quantify the nutrient stress from F_v/F_m alone (Gorbunov & Falkowski 2021). Also, both iron and nitrogen limitation lead to a decrease in F_v/F_m (**Table 2**) that requires the development of additional, stress-specific indicators (or a suite of indicators) for quantitative diagnostics of iron and nitrogen limitation in the ocean.

In contrast to F_v/F_m, the kinetic fluorescence parameters, such as the time of Q_A reoxidation (t_{Q_A}) and photosynthetic turnover rates, show a striking difference between iron and nitrogen stress (**Table 2**). While nitrogen limitation does not affect t_{Q_A} (Gorbunov & Falkowski 2021), iron stress leads to a strong increase in t_{Q_A} (Greene et al. 1992, data from Lin et al. 2016) (**Figure 1**). This increase in t_{Q_A} under iron stress is caused by a decrease in the amount of the iron-rich cofactors of the electron transport chain in PSII (Greene et al. 1992, Behrenfeld & Milligan 2013). It should be noted that the measured t_{Q_A} values are affected by the redox state of the plastoquinone pool (e.g., Gorbunov & Falkowski 2021). For instance, when the plastoquinone pool becomes reduced (e.g., under saturating irradiance), t_{Q_A} increases dramatically (Gorbunov & Falkowski 2021). The plastoquinone pool may be reduced even in darkness due to chlororespiration, and this effect is observed in some algae even under nitrogen-replete conditions (Bennoun 1982). To avoid this potential artifact, t_{Q_A} must be recorded when the plastoquinone pool is oxidized.

In contrast to t_{Q_A}, the photosynthetic turnover rates ($1/\tau$) show the opposite trend in relation to nitrogen and iron stress (**Table 2**). Nitrogen limitation has a strong impact on the Calvin–Benson–Bassham cycle and RuBisCO activity (Geider et al. 1993). As a result, the maximum photosynthetic ETRs (ETR_{max}) achieved under saturating irradiance and photosynthetic turnover rates are significantly reduced, and this reduction is much greater than the decrease in the maximum quantum yield of photochemistry in PSII, F_v/F_m (Gorbunov & Falkowski 2021). Furthermore, this decrease in $1/\tau$ follows a linear dependence with growth rates (Gorbunov & Falkowski 2021). Measurements of photosynthetic turnover rates can be done by kinetic analysis of Q_A reoxidation under saturating irradiance. This kinetic analysis has been implemented in mini-FIRe instruments and offers a tool for quantitative diagnostics of nitrogen limitation and its impact on growth rates and rates of net primary production (Gorbunov & Falkowski 2021).

Iron stress leads to a marked decrease in the maximum quantum yield of photochemistry in PSII, F_v/F_m (Greene et al. 1992, Boyd et al. 2001, Coale et al. 2004), that is accompanied by a dramatic increase in fluorescence lifetimes. In regions with severe iron stress, such as high-nutrient, low-chlorophyll regions of the Southern Ocean and equatorial Pacific, F_v/F_m values are as low as 0.2–0.3, and the lifetimes are >2.0 ns (Lin et al. 2016). Such long lifetimes are not observed in nitrogen-stressed phytoplankton (Lin et al. 2016). These low F_v/F_m values and extremely long lifetimes suggest that there is a significant fraction of nonfunctional PSII reaction centers and energetically uncoupled antenna pigment–protein complexes (Vassiliev et al. 1995, Schrader et al. 2011). The uncoupled antenna pigment–protein complexes exhibit a fluorescence lifetime of ~4.0 ns (Morales et al. 2001), which is much longer than the lifetimes of in vivo chlorophyll fluorescence in cells with fully closed reaction centers (i.e., at the F_m level). The combination of lifetime measurements and variable fluorescence allows one to separate signals from nonfunctional reaction centers and uncoupled antennae and to determine the fraction of uncoupled antennae in iron-stressed phytoplankton (Falkowski et al. 2017, Park et al. 2017). In severely

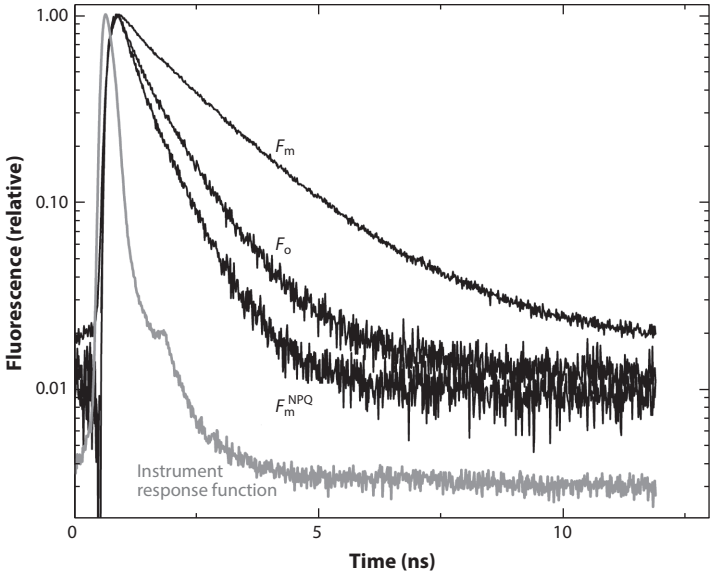

Figure 5

The concept of picosecond lifetime measurements. Fluorescence is induced by an ultrashort laser pulse, and the decay kinetics is recorded on pico- and nanosecond timescales. The rate of fluorescence decay (i.e., lifetime) is directly proportional to the absolute quantum yield of fluorescence. The three profiles show the fluorescence kinetics of phytoplankton at different physiological states of photosystem II reaction centers. F_o was recorded in dark-adapted cells with open reaction centers (when the quantum yield of photochemistry is maximum), F_m in dark-adapted cells with closed centers (when photochemistry is nil), and F_m^{NPQ} under high-light exposure with closed centers. The reduction in the fluorescence lifetime under high light is due to nonphotochemical quenching. The gray trace is the instrument response function.

iron-limited phytoplankton communities of the Southern Ocean, as much as 30–40% of antennae are energetically uncoupled (Park et al. 2017, Sherman et al. 2020).

THE THEORETICAL BASIS OF FLUORESCENCE QUANTUM YIELDS AND LIFETIMES

What, then, is the fate of photons that are absorbed by phytoplankton in the world's oceans? Using amplitude-based fluorescence analyses, we have shown how F_v/F_m measured with a saturating single turnover flash can yield ϕ_P in Equation 1. Can we solve for one of the other two yields and determine the energy distribution of absorbed photons?

Fluorescence is a delayed light emission process that is described by one or more exponential decay functions that can be parameterized by the lifetime, which is the e-folding time of the decay function. The fluorescence lifetime can be quantitatively related to the absolute quantum yield of fluorescence (Lakowicz 2006):

$$\phi_f = \tau/\tau_n, \qquad 18.$$

where τ is the observed lifetime (not to be confused with the photosynthetic turnover time), and τ_n is the intrinsic (or natural) lifetime, which is a constant for the molecule. Thus, the longer the lifetime is, the higher the quantum yield of fluorescence is. Note that the fluorescence lifetime (τ) is deduced from picosecond kinetic analysis (**Figure 5**), which is a different technique than the FRR/FIRe analysis of micro- and millisecond relaxation kinetics of Q_A reoxidation (**Figure 1**).

The natural lifetime (τ_n) is that which would be observed if fluorescence emission were the only path of dissipation of excited state energy; this number cannot be measured directly. The calculated value of τ_n for chlorophyll *a* is 15 ns (Brody & Rabinowitch 1957). In a population of molecules, the actual measured lifetimes are inevitably shorter than the natural lifetime due to intramolecular conversion (i.e., energy dissipation as heat) and triplet state formation. The actual measured lifetimes of isolated chlorophyll *a* molecules range from approximately 3.0 to 5.1 ns, depending on solvent polarity. These measured lifetimes correspond to quantum yields ranging from 20% to 32%. Fluorescence lifetimes in living cells are much shorter (approximately 0.3 to 1.5 ns), as a significant fraction of the absorbed energy is used in photochemical reactions, and reflect the physiological state of the cells (Lin et al. 2016, Falkowski et al. 2017).

PHYSIOLOGICAL INFORMATION FROM PICOSECOND FLUORESCENCE KINETICS

The kinetics of chlorophyll *a* fluorescence lifetimes in living cells follows a multicomponent exponential decay (**Figure 5**). The multicomponent nature of in vivo chlorophyll fluorescence reflects the rates of energy migration in antenna complexes and photochemical reactions in the PSII core (Holzwarth 1986).

The complexity of in vivo chlorophyll fluorescence can be described by exciton–radical pair equilibrium kinetic models (Schatz et al. 1988). These models consider energy migration in the PSII antenna–reaction center complex on ultrafast, picosecond timescales. These energy migration processes include charge separation in reaction centers, charge recombination, and the first, ultrafast, step of the electron transfer. **Figure 6** shows an example of an exciton–radical pair equilibrium kinetic model. Upon excitation of the PSII antenna, a rapid excitation equilibrium (faster than 10 ps) (Holzwarth et al. 2006) is achieved between the antenna and the reaction centers (denoted as A*/RC*). The exciton exchange between the antenna and reaction center is described by the rate constants for exciton trapping (k_t) and back recombination (k_{-t}). Due to this rapid equilibrium, exciton–radical pair equilibrium models usually assume that the excited states of the antenna and reaction centers are not separated and are, therefore, represented by only one compartment (**Figure 6**). The next step in energy migration is charge separation in the reaction center (with the rate constant k_1) that results in the formation of a radical pair, $P680^+I^-$. There are four major pathways of energy conversion and recombination of the radical pair. First, the pair could recombine to the antenna/reaction center excited state (with the rate constant k_{-1}). Alternatively, it may recombine (through nonradiative decay) to the ground state (k_{2D}) or the triplet excited state of P680 (k_{2T}, spin dephasing), or it could transfer an electron to Q_A (k_{2Q}, charge

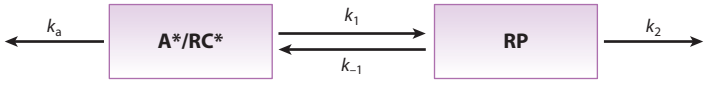

Figure 6

An exciton–radical pair equilibrium kinetic model used for analysis of the picosecond kinetics of in vivo chlorophyll fluorescence. The rate constants of the reactions are determined from the analysis of the experimental picosecond time-resolved fluorescence kinetics, in combination with variable fluorescence measurements. Abbreviations: A, light-harvesting antenna; RC, reaction center; RP, radical pair [P^+I^-] (which is produced in the reaction center as a result of charge separation); k_a, antenna deactivation rate constant (due to fluorescence and thermal dissipation); k_1, rate constant of charge separation; k_{-1}, rate constant of charge recombination; k_2, rate of nonphotochemical losses (due to spin conversion to the triplet state $^3[P^+I^-]$ and nonradiative charge recombination). Asterisks indicate that the antenna and reaction center complex is in the excited state. Figure adapted with permission from Schatz et al. (1988).

stabilization). Charge stabilization takes place in open reaction centers, whereas the other two pathways dominate in closed reaction centers. Deactivation of the excited states in the antenna complex is represented by nonradiative (thermal dissipation, k_{DA}) and radiative (fluorescence, k_F) processes.

Using a combination of amplitude-based and lifetime fluorometers over thousands of kilometers of the world's oceans, Lin et al. (2016) calculated the average quantum yield for photochemistry in PSII as 0.35 and the average quantum yield for chlorophyll *a* fluorescence as 0.07. These results suggest that, on average, approximately 60% of the photons absorbed by phytoplankton in the upper ocean are dissipated as heat. Hence, although phytoplankton photosynthesis can obtain a quantum yield of 0.65 under nutrient-complete conditions, in the real world they function at a much lower efficiency.

PHYTOPLANKTON PHYSIOLOGY FROM SPACE: VALIDATION AND CALIBRATION OF SOLAR-INDUCED CHLOROPHYLL FLUORESCENCE YIELDS

Variable fluorescence signals can only be recorded from space with high-power lasers or some other source of pulsed light, which is not practical. An alternative approach to infer phytoplankton physiology and photosynthetic rates is based on measurements of the absolute quantum yields of solar-induced chlorophyll *a* fluorescence (Lin et al. 2016, Falkowski et al. 2017). With the launch of the Moderate Resolution Imaging Spectroradiometer (MODIS) and Medium Resolution Imaging Spectrometer (MERIS) satellites and upcoming NASA missions such as the Plankton, Aerosol, Cloud, Ocean Ecosystem (PACE) mission, which can detect solar-induced chlorophyll fluorescence signals from the global ocean, it became theoretically possible to calculate the quantum yield of chlorophyll fluorescence from space (Abbott & Letelier 1999, Behrenfeld et al. 2009, Huot et al. 2013).

The MODIS/MERIS analytical algorithms retrieve the quantum yields of chlorophyll fluorescence from the ratio of two independent variables: the magnitude of solar-induced fluorescence and the number of quanta absorbed by phytoplankton. The logic of these algorithms is based on the physics of water-leaving radiance from the oceans. Seawater scatters solar radiation to the inverse 4.3 power of wavelength. This is not Rayleigh scattering but rather fluctuation density scattering (Morel & Prieur 1977, Falkowski & Raven 2007). The decay of radiation from the ocean as a function of wavelength is modified by molecules that absorb the inbound and outbound light. To first order, the Soret band of chlorophylls absorbs blue light and makes the ocean darker. Algorithms that retrieve chlorophyll concentrations from satellite measurements of ocean color are based in this phenomenon (Morel & Prieur 1977, Gordon & Morel 1983, Gordon et al. 1988, Esaias et al. 1998, Gower et al. 1999, McClain 2009). In addition, however, solar radiation can induce chlorophyll fluorescence (solar-induced fluorescence, also called passive fluorescence). This phenomenon is detected as a red peak (centered at ~683 nm) in the spectra of water-leaving radiance (Neville & Gower 1977, Gordon et al. 1988, Gower et al. 1999). That signal is recorded as a fluorescence line height (Abbott & Letelier 1998, 1999), which is observed as a source of red photons emitted back to space over the background of the water-leaving radiance. Indeed, solar-induced fluorescence is the only signal that is emitted from the ocean and detectable from space that can be unambiguously ascribed to life on Earth (Cullen et al. 1997, Behrenfeld et al. 2009). By dividing the solar-induced fluorescence line height by the concentration of chlorophyll, obtained from the change in ocean color, one can derive the quantum yield of fluorescence from satellites (Behrenfeld et al. 2009; Huot et al. 2005, 2013).

The natural variations of fluorescence yields are the sources of both errors and useful information. Solar-induced fluorescence yield is highly variable in nature (Cullen et al. 1997, Letelier

et al. 1997, Abbott & Letelier 1998, Maritorena et al. 2000, Morrison 2003, Huot et al. 2005). While the apparently huge variability of chlorophyll fluorescence yield in the ocean (~10-fold) is often correlated with environmental forcing (Letelier et al. 1997, Huot et al. 2005, Behrenfeld et al. 2009, Lin et al. 2016), the mechanisms and interpretation of this relationship remain to be elucidated.

The development of remote sensing algorithms for interpretation of the quantum yields of solar-induced fluorescence crucially depends on comparison with accurate in situ measurements of the quantum yields. The quantum yields cannot be measured by using variable fluorescence instruments but can be measured by using picosecond fluorescence kinetics (Lin et al. 2016). Seagoing instruments have been designed to continuously measure chlorophyll lifetimes in real time without having to concentrate phytoplankton. Such measurements are the only way to verify satellite-derived estimates of solar-induced fluorescence yields (Lin et al. 2016).

CONCLUSIONS

Over the past few decades, the theoretical basis of changes in chlorophyll fluorescence in living phytoplankton facilitated experimental research that has fundamentally changed the interpretation of the biological responses to ocean physics. Technological advances in ultrafast laser diodes, high-intensity light-emitting diodes, ultrahigh-resolution photon detectors, and sophisticated miniature computers have allowed the development of seagoing instruments that can measure, with extremely high accuracy and precision, variations in chlorophyll fluorescence kinetics and lifetimes. This is a long way from radiocarbon isotope analyses, an approach that was pervasive from the 1960s through the early part of the twenty-first century, in understanding primary production in the world's oceans. We hope that this review gives the reader insight into the degree to which in situ chlorophyll fluorescence measurements can lead to an understanding of photosynthetic physiology in the world's oceans nondestructively and in real time.

DISCLOSURE STATEMENT

The authors are not aware of any affiliations, memberships, funding, or financial holdings that might be perceived as affecting the objectivity of this review.

ACKNOWLEDGMENTS

This research was supported by the NASA Ocean Biology and Biogeochemistry Program (grants NNX16AT54G and 80NSSC18K1416). We thank Hartmut Lichtenthaller for a historical perspective and Zbignew Kolber, David Suggett, Philippe Tortell, Nina Schuback, Kevin Oxborough, Mark Moore, and members of Scientific Committee on Oceanic Research working group 156 on active chlorophyll fluorescence for autonomous measurements of global marine primary productivity for discussion. We also thank the *Annual Review of Marine Science* Editorial Committee for the opportunity to provide this review.

LITERATURE CITED

Abbott MR, Letelier RM. 1998. Decorrelation scales of chlorophyll as observed from bio-optical drifters in the California Current. *Deep-Sea Res. II* 45:1639–67

Abbott MR, Letelier RM. 1999. *Algorithm theoretical basis document: chlorophyll fluorescence (MODIS product number 20)*. Rep., Ocean Biol. Process. Group, Goddard Space Cent., Natl. Aeronaut. Space Adm., Greenbelt, MD

Abbott MR, Richerson PJ, Powell TM. 1982. In situ response of phytoplankton fluorescence to rapid variations in light. *Limnol. Oceanogr.* 27:218–25
Bailleul B, Cardol P, Breyton C, Finazzi G. 2010. Electrochromism: a useful probe to study algal photosynthesis. *Photosynth. Res.* 106:179
Behrenfeld MJ, Bale A, Kolber ZS, Aiken J, Falkowski P. 1996. Confirmation of iron limitation of phytoplankton photosynthesis in the equatorial Pacific. *Nature* 383:508–11
Behrenfeld MJ, Falkowski PG. 1997. Photosynthetic rates derived from satellite-based chlorophyll concentration. *Limnol. Oceanogr.* 42:1–20
Behrenfeld MJ, Kolber ZS. 1999. Widespread iron limitation of phytoplankton in the South Pacific Ocean. *Science* 283:840–43
Behrenfeld MJ, Milligan AJ. 2013. Photophysiological expressions of iron stress in phytoplankton. *Annu. Rev. Mar. Sci.* 5:217–46
Behrenfeld MJ, Westberry TK, Boss ES, O'Malley RT, Siegel DA, et al. 2009. Satellite-detected fluorescence reveals global physiology of ocean phytoplankton. *Biogeosciences* 6:779–94
Behrenfeld MJ, Worthington K, Sherrell RM, Chavez FP, Strutton P, et al. 2006. Controls on tropical Pacific Ocean productivity revealed through nutrient stress diagnostics. *Nature* 442:1025–28
Bennoun P. 1982. Evidence for a respiratory chain in the chloroplast. *PNAS* 79:4352–56
Bilger W, Bjorkman O. 1990. Role of the xanthophyll cycle in photoprotection elucidated by measurements of light-induced absorption changes, fluorescence and photosynthesis in Hedera canariensis. *Photosynth. Res.* 25:173–85
Bonnet S, Guieu C, Bruyant F, Prasil O, Van Wambeke F, et al. 2008. Nutrient limitation of primary productivity in the Southeast Pacific (BIOSOPE cruise). *Biogeosciences* 5:215–25
Bowes J, Crofts AR. 1980. Binary oscillations in the rate of reoxidation of the primary acceptor of Photosystem II. *Biochim. Biophys. Acta* 590:373–84
Boyd PW, Abraham ER. 2001. Iron-mediated changes in phytoplankton photosynthetic competence during SOIREE. *Deep-Sea Res. II* 48:2529–50
Boyd PW, Crossley AC, DiTullio GR, Griffiths FB, Hutchins DA, et al. 2001. Control of phytoplankton growth by iron supply and irradiance in the subantarctic Southern Ocean: experimental results from the SAZ Project. *J. Geophys. Res.* 106:31573–83
Boyd PW, Jickells T, Law CS, Blain S, Boyle EA, et al. 2007. Mesoscale iron enrichment experiments 1993–2005: synthesis and future directions. *Science* 315:612–17
Boyd PW, Wong CS, Merrill J, Whitney F, Snow J, et al. 1998. Atmospheric iron supply and enhanced vertical carbon flux in the NE subarctic Pacific: Is there a connection? *Glob. Biogeochem. Cycles* 12:429–41
Brewster D. 1834. On the colours of natural bodies. *Trans. R. Soc. Edinb.* 12:538–45
Brody SS, Rabinowitch E. 1957. Excitation lifetime of photosynthetic pigments in vitro and in vivo. *Science* 125:555
Brown BE, Ambarsari I, Warner ME, Fitt WK, Dunne RP, et al. 1999. Diurnal changes in photochemical efficiency and xanthophyll concentrations in shallow water reef corals: evidence for photoinhibition and photoprotection. *Coral Reefs* 18:99–105
Buck JM, Sherman J, Bártulos CR, Serif M, Halder M et al. 2019. Lhcx proteins provide photoprotection via thermal dissipation of absorbed light in the diatom *Phaeodactylum tricornutum*. *Nat. Commun.* 10:4167
Butler WL. 1972. On the primary nature of fluorescence yield changes associated with photosynthesis. *PNAS* 69:3420–22
Butler WL. 1978. Energy distribution in the photochemical apparatus of photosynthesis. *Annu. Rev. Plant Physiol.* 29:345–78
Campbell DA, Hurry V, Clarke A, Gustafsson P, Oquist G. 1998. Chlorophyll fluorescence analysis of cyanobacterial photosynthesis and acclimation. *Microbiol. Mol. Biol. Rev.* 62:667–83
Campbell DA, Tyystjärvi E. 2012. Parameterization of photosystem II photoinactivation and repair. *Biochim. Biophys. Acta* 1817:258–65
Coale KH, Johnson KS, Chavez FP, Buesseler KO, Barber RT et al. 2004. Southern ocean iron enrichment experiment: carbon cycling in high- and low-Si waters. *Science* 304:408–14
Crofts AR, Wright CA. 1983. The electrochemical domain of photosynthesis. *Biochim. Biophys. Acta* 726:149–85

Cullen JJ, Ciotti AM, Davis RF, Neale PJ. 1997. Relationship between near-surface chlorophyll and solar-stimulated fluorescence: biological effects. In *Ocean Optics XIII*, ed. SG Ackleson, RJ Frouin, pp. 272–77. Proc. SPIE 2963. Bellingham, WA: Soc. Photo-Opt. Instrum. Eng.

Demers S, Roy S, Gagnon R, Vignault C. 1991. Rapid light-induced changes in cell fluorescence and in xanthophyll-cycle pigments of *Alexandrium excavatum* (Dinophyceae) and *Thalassiosira pseudonana* (Bacillariophyceae): a photo-protection mechanism. *Mar. Ecol. Prog. Ser.* 76:185–93

Demmig-Adams B, Adams WW III. 1996. The role of xanthophyll cycle carotenoids in the protection of photosynthesis. *Trends Plant Sci*. 1:21–26

Demmig-Adams B, Garab G, Adams WW III, Govindjee, eds. 2014. *Non-Photochemical Quenching and Energy Dissipation in Plants, Algae and Cyanobacteria*. Dordrecht, Neth.: Springer

Dugdale RC. 1967. Nutrient limitation in the sea: dynamics, identification, and significance. *Limnol. Oceanogr.* 12:685–95

Duysens LNM. 1956. Energy transformations in photosynthesis. *Annu. Rev. Plant Physiol.* 7:25–50

Duysens LNM, Amesz J, Kamp BM. 1961. Two photochemical systems in photosynthesis. *Nature* 190:510–11

Duysens LNM, Sweers HE. 1963. Mechanism of two photochemical reactions in algae as studied by means of fluorescence. In *Studies on Microalgae and Photosynthetic Bacteria*, ed. Jpn. Soc. Plant Physiol., pp. 353–72. Tokyo: Univ. Tokyo Press

El-Bissati K, Delphin E, Murata N, Etienne AL, Kirilovsky D. 2000. Photosystem II fluorescence quenching in the cyanobacterium *Synechocystis* sp. PCC 6803: involvement of two different mechanisms. *Biochim. Biophys. Acta* 1457:229–42

Emerson R. 1957. Dependence of yield of photosynthesis in long wave red on wavelength and intensity of supplementary light. *Science* 125:746–52

Eppley RW. 1980. Estimating phytoplankton growth rates in the central oligotrophic oceans. In *Primary Productivity in the Sea*, ed. PG Falkowski, pp. 231–42. New York: Plenum

Esaias WE, Abbott MR, Barton I, Brown OB, Campbell JW, et al. 1998. An overview of MODIS capabilities for ocean science observations. *IEEE Trans. Geosci. Remote Sens.* 36:1250–65

Falkowski PG, Dubinsky Z, Wyman K. 1985. Growth-irradiance relationships in phytoplankton. *Limnol. Oceanogr.* 30:311–21

Falkowski PG, Koblizek M, Gorbunov MY, Kolber ZS. 2004. Development and application of variable chlorophyll fluorescence techniques in marine ecosystems. See Papageorgiou & Govindjee 2004, pp. 757–78

Falkowski PG, Kolber ZS. 1995. Variations in the chlorophyll fluorescence yields in the phytoplankton in the world oceans. *Aust. J. Plant Physiol.* 22:341–55

Falkowski PG, Lin H, Gorbunov MY. 2017. What limits photosynthetic energy conversion efficiency in nature? Lessons from the oceans. *Philos. Trans. R. Soc. B* 372:20160376

Falkowski PG, Raven JA. 2007. *Aquatic Photosynthesis*. Princeton, NJ: Princeton Univ. Press. 2nd ed.

Falkowski PG, Wyman K, Ley AC, Mauzerall DC. 1986. Relationship of steady state photosynthesis to fluorescence in eukaryotic algae. *Biochim. Biophys. Acta* 849:183–92

Geider RJ, LaRoche J, Greene RM, Olaizola M. 1993. Response of the photosynthetic apparatus of *Phaeodactylum tricornutum* (Bacillariophyceae) to nitrate, phosphate, or iron starvation. *J. Phycol.* 29:755–66

Genty B, Briantais JM, Baker NR. 1989. The relationship between the quantum yield of photosynthetic electron transport and quenching of chlorophyll fluorescence. *Biochim. Biophys. Acta* 990:87–92

Gervais F, Riebesell U, Gorbunov MY. 2002. Changes in primary productivity and chlorophyll *a* in response to iron fertilization in the Southern Polar Frontal Zone. *Limnol. Oceanogr.* 47:1324–35

Gorbunov MY, Chekalyuk AM. 1992. Lidar in-situ study of sunlight regulation of phytoplankton photosynthetic activity and chlorophyll fluorescence. In *Laser Study of Macroscopic Biosystems*, ed. JE Korppi-Tommola, pp. 421–27. Proc. SPIE 1922. Bellingham, WA: Soc. Photo-Opt. Instrum. Eng.

Gorbunov MY, Falkowski PG. 2005. Fluorescence induction and relaxation (FIRe) technique and instrumentation for monitoring photosynthetic processes and primary production in aquatic ecosystems. In *Photosynthesis: Fundamental Aspects to Global Perspectives; Proceedings of the 13th International Congress on Photosynthesis*, ed. A van der Est, D Bruce, pp. 1029–31. Lawrence, KS: Alliance Commun. Group

Gorbunov MY, Falkowski PG. 2021. Using chlorophyll fluorescence kinetics to determine photosynthesis in aquatic ecosystems. *Limnol. Oceanogr.* 66:1–13

Gorbunov MY, Falkowski PG, Kolber ZS. 2000. Measurement of photosynthetic parameters in benthic organisms in situ using a SCUBA-based fast repetition rate fluorometer. *Limnol. Oceanogr.* 45:242–45

Gorbunov MY, Kolber ZS, Falkowski PG. 1999. Measuring photosynthetic parameters in individual algal cells by Fast Repetition Rate fluorometry. *Photosynth. Res.* 62:141–53

Gorbunov MY, Kolber ZS, Lesser MP, Falkowski PG. 2001. Photosynthesis and photoprotection in symbiotic corals. *Limnol. Oceanogr.* 46:75–85

Gorbunov MY, Kuzminov FI, Fadeev VV, Kim JD, Falkowski PG. 2011. A kinetic model of non-photochemical quenching in cyanobacteria. *Biochim. Biophys. Acta* 1807:1591–99

Gorbunov MY, Shirsin E, Nikonova E, Fadeev VV, Falkowski PG. 2020. A multi-spectral fluorescence induction and relaxation (FIRe) technique for physiological and taxonomic analysis of phytoplankton communities. *Mar. Ecol. Prog. Ser.* 644:1–13

Gordon HR, Brown OB, Evans RH, Brown JW, Smith RC, et al. 1988. A semianalytic radiance model of ocean color. *J. Geophys. Res. Atmos.* 93:10909–24

Gordon HR, Morel AY. 1983. In-water algorithms. In *Remote Assessment of Ocean Color for Interpretation of Satellite Visible Imagery: A Review*, pp. 24–67. New York: Springer

Govindjee. 1995. Sixty-three years since Kautsky: chlorophyll *a* fluorescence. *Aust. J. Plant Physiol.* 22:131–60

Gower JFR, Doerffer R, Borstad GA. 1999. Interpretation of the 685 nm peak in water-leaving radiance spectra in terms of fluorescence, absorption and scattering, and its observation by MERIS. *Int. J. Remote Sens.* 20:1771–86

Greene RM, Geider RJ, Kolber ZS, Falkowski PG. 1992. Iron-induced changes in light harvesting and photochemical energy conversion processes in eukaryotic marine algae. *Plant Physiol.* 100:565–75

Hendrickson L, Furbank RT, Chow WS. 2004. A simple alternative approach to assessing the fate of absorbed light energy using chlorophyll fluorescence. *Photosynth. Res.* 82:73

Herron HA, Mauzerall D. 1971. The development of photosynthesis in a greening mutant of *Chlorella* and an analysis of the light saturation curve. *Plant Physiol.* 50:141–48

Holzwarth AR. 1986. Fluorescence lifetimes in photosynthetic systems. *Photochem. Photobiol.* 43:707–25

Holzwarth AR, Müller MG, Reus M, Nowaczyk M, Sander J, Rögner M. 2006. Kinetics and mechanism of electron transfer in intact photosystem II and in the isolated reaction center: pheophytin is the primary electron acceptor. *PNAS* 103:6895–900

Horton P, Ruban AV, Walters R. 1996. Regulation of light harvesting in green plants. *Annu. Rev. Plant Physiol. Plant Mol. Biol.* 47:655–84

Hughes DJ, Campbell DA, Doblin MA, Kromkamp JC, Lawrenz EC, et al. 2018a. Roadmaps and detours: active chlorophyll-*a* assessments of primary productivity across marine and freshwater systems. *Environ. Sci. Technol.* 52:12039–54

Hughes DJ, Varkey D, Doblin MA, Ingleton T, McInnes A, et al. 2018b. Impact of nitrogen availability upon the electron requirement for carbon fixation in Australian coastal phytoplankton communities. *Limnol. Oceanogr.* 63:1891–910

Huot Y, Brown CA, Cullen JJ. 2005. New algorithms for MODIS sun-induced chlorophyll fluorescence and a comparison with present data products. *Limnol. Oceanogr. Methods* 3:108–30

Huot Y, Franz BA, Fradette M. 2013. Estimating variability in the quantum yield of sun-induced chlorophyll fluorescence: a global analysis of oceanic waters. *Remote Sens. Environ.* 132:238–53

Joliot P, Joliot A. 2003. Excitation transfer between photosynthetic units: the 1964 experiment. *Photosynth Res.* 76:241–45

Kautsky H, Hirsch A. 1931. Neue Versuche zur Kohlensauerassimilation. *Naturwissenschaften* 48:964

Ke B. 2001. Phycobiliproteins and phycobilisomes. In *Photosynthesis: Photobiochemistry and Photobiophysics*, pp. 251–69. Dordrecht, Neth.: Kluwer Acad.

Kiefer DA. 1973. Fluorescence properties of natural phytoplankton populations. *Mar. Biol.* 22:263–69

Kirilovsky D, Kerfeld C. 2016. Cyanobacterial photoprotection by the orange carotenoid protein. *Nat. Plants* 2:16180

Ko E, Gorbunov MY, Jung J, Joo HM, Lee Y, et al. 2020. Effects of nitrogen limitation on phytoplankton physiology in the western Arctic Ocean in summer. *J. Geophys. Res. Oceans* 125:ee2020JC016501

Ko E, Park J, Gorbunov MY, Yoo S. 2019. Uncertainties in variable fluorescence and ^{14}C methods to estimate primary productivity: a case study in the coastal waters off the Korean peninsula. *Mar. Ecol. Prog. Ser.* 627:13–31

Kolber ZS, Barber RT, Coale KH, Fitzwater SE, Greene RM, et al. 1994. Iron limitation of phytoplankton photosynthesis in the equatorial Pacific Ocean. *Nature* 371:145–49

Kolber ZS, Falkowski PG. 1993. Use of active fluorescence to estimate phytoplankton photosynthesis in situ. *Limnol. Oceanogr.* 38:1646–65

Kolber ZS, Prasil O, Falkowski PG. 1998. Measurements of variable chlorophyll fluorescence using fast repetition rate techniques: defining methodology and experimental protocols. *Biochim. Biophys. Acta* 1376:88–106

Kolber ZS, Zehr J, Falkowski PG. 1988. Effects of growth irradiance and nitrogen limitation on photosynthetic energy conversion in photosystem II. *Plant Physiol.* 88:72–79

Kramer DM, DiMarco G, Loreto F. 1995. Contribution of plastoquinone quenching to saturation pulse-induced rise of chlorophyll fluorescence in leaves. In *Photosynthesis: From Light to the Biosphere*, Vol. 1, ed. P Mathis, pp. 147–50. Dordrecht, Neth.: Kluwer Acad.

Kramer DM, Johnson G, Kiirats O, Edwards GE. 2004. New fluorescence parameters for the determination of QA redox state and excitation energy fluxes. *Photosynth. Res.* 79:209–18

Kromkamp JC, Dijkman NA, Peene J, Simis SGH, Gons HJ. 2008. Estimating phytoplankton primary production in Lake Ijsselmeer (the Netherlands) using variable fluorescence (PAM-FRRF) and C-uptake techniques. *Eur. J. Phycol.* 43:327–44

Kulk G, van de Poll WH, Buma AGJ. 2018. Photophysiology of nitrate limited phytoplankton communities in Kongsfjorden, Spitsbergen. *Limnol. Oceanogr.* 63:2606–17

Kuzminov FI, Gorbunov MY. 2016. Energy dissipation pathways in Photosystem 2 of the diatom, *Phaeodactylum tricornutum*, under high light conditions. *Photosynth. Res.* 127:219–35

Lakowicz JR. 2006. *Principles of Fluorescence Spectroscopy*. New York: Springer. 3rd ed.

Lawrenz E, Silsbe G, Capuzzo E, Ylostalo P, Forster RM, et al. 2013. Predicting the electron requirement for carbon fixation in seas and oceans. *PLOS ONE* 8:e58137

Laws EA. 1991. Photosynthetic quotients, new production and net community production in the open ocean. *Deep-Sea Res. I* 38:143–67

Letelier RM, Abbott MR, Karl DM. 1997. Chlorophyll natural fluorescence response to upwelling events in the Southern Ocean. *Geophys. Res. Lett.* 24:409–12

Lewis KM, Arntsen AE, Coupel P, Joy-Warren H, Lowry KE, et al. 2019. Photoacclimation of Arctic Ocean phytoplankton to shifting light and nutrient limitation. *Limnol. Oceanogr.* 64:284–301

Ley AC, Mauzerall D. 1982. Absolute absorption cross sections for Photosystem II and the minimum quantum requirement for photosynthesis in *Chlorella vulgaris*. *Biochim. Biophys. Acta* 680:95–106

Ley AC, Mauzerall D. 1986. The extent of energy transfer among Photosystem II reaction centers in *Chlorella*. *Biochim. Biophys. Acta* 850:234–48

Lichtenthaler HK. 1992. The Kautsky effect: 60 years of chlorophyll fluorescence induction kinetics. *Photosynthetica* 27:44–55

Lin H, Kuzminov FI, Park J, Lee SH, Falkowski PG, et al. 2016. The fate of photons absorbed by phytoplankton in the global ocean. *Science* 351:264–67

Litchman E, Klausmeier CA. 2008. Trait-based community ecology of phytoplankton. *Annu. Rev. Ecol. Evol. Syst.* 39:615–39

Long SP, Humphries S, Falkowski PG. 1994. Photoinhibition of photosynthesis in nature. *Annu. Rev. Plant Physiol. Plant Mol. Biol.* 45:633–62

MacColl R. 1998. Cyanobacterial phycobilisomes. *J. Struct. Biol.* 124:311–34

Maritorena S, Morel A, Gentili B. 2000. Determination of the fluorescence quantum yield by oceanic phytoplankton in their natural habitat. *Appl. Opt.* 39:6725–37

Mauzerall D. 1972. Light-induced changes in *Chlorella*, and the primary photoreaction for the production of oxygen. *PNAS* 69:1358–62

Mauzerall D. 1986. The optical cross section and the absolute size of a photosynthetic unit. *Photosynth. Res.* 10:163–70

McClain CR. 2009. A decade of satellite ocean color observations. *Annu. Rev. Mar. Sci.* 1:19–42
McElroy MB. 1983. Marine biological controls on atmospheric CO_2 and climate. *Nature* 302:328–29
Mills MM, Brown ZW, Laney SR, Ortega-Retuerta E, Lowry KE, et al. 2018. Nitrogen limitation of the summer phytoplankton and heterotrophic prokaryote communities in the Chukchi Sea. *Front. Mar. Sci.* 5:362
Mitchell P. 1977. Vectorial chemiosmotic processes. *Annu. Rev. Biochem.* 46:996–1005
Moore CM, Mills MM, Arrigo KR, Berman-Frank I, Bopp L, et al. 2013. Processes and patterns of oceanic nutrient limitation. *Nat. Geosci.* 6:701–10
Morales F, Moise N, Quilez R, Abadia A, Abadia J, et al. 2001. Iron deficiency interrupts energy transfer from a disconnected part of the antenna to the rest of Photosystem II. *Photosynth. Res.* 70:207–20
Morel A, Prieur L. 1977. Analysis of variations in ocean color. *Limnol. Oceanogr.* 22:709–22
Morrison JR. 2003. In situ determination of the quantum yield of phytoplankton chlorophyll *a* fluorescence: a simple algorithm, observations, and a model. *Limnol. Oceanogr.* 48:618–31
Myers J, Graham JR. 1971. The photosynthetic unit of *Chlorella* measured by repetitive short flashes. *Plant Physiol.* 48:282–86
Neville RA, Gower JFR. 1977. Passive remote sensing of phytoplankton via chlorophyll *a* fluorescence. *J. Geophys. Res.* 82:3487–93
Nielsdottir MC, Moore CM, Sanders R, Hinz DJ, Achterberg EP. 2009. Iron limitation of the postbloom phytoplankton communities in the Iceland Basin. *Glob. Biogeochem. Cycles* 23:GB3001
Olaizola M, LaRoche J, Kolber ZS, Falkowski PG. 1994. Nonphotochemical fluorescence quenching and the diadinoxanthin cycle in a marine diatom. *Photosynth. Res.* 41:357–70
Olson RJ, Sosik HM, Chekalyuk AM, Shalapyonok A. 2000. Effects of iron enrichment on phytoplankton in the Southern Ocean during late summer: active fluorescence and flow cytometric analyses. *Deep-Sea Res. II* 47:3181–200
Oxborough K, Moore CM, Suggett DJ, Lawson T, Chan HG, et al. 2012. Direct estimation of functional PSII reaction center concentration and PSII electron flux on a volume basis: a new approach to the analysis of Fast Repetition Rate fluorometry (FRRf) data. *Limnol. Oceanogr. Methods* 10:142–54
Paillotin G. 1976. Capture frequency excitation and energy transfer between photosynthetic units in the photosystem II. *J. Theor. Biol.* 58:219–35
Papageorgiou GC, Govindjee, eds. 2004. *Chlorophyll a Fluorescence: A Signature of Photosynthesis*. Dordrecht, Neth.: Springer
Park J, Kuzminov FI, Bailleul B, Yang EJ, Lee SH, et al. 2017. Light availability rather than Fe controls the magnitude of massive phytoplankton blooms in the Amundsen Sea polynyas, Antarctica. *Limnol. Oceanogr.* 62:2260–76
Parkhill JP, Maillet G, Cullen JJ. 2001. Fluorescence-based maximal quantum yield for PSII as a diagnostic of nutrient stress. *J. Phycol.* 37:517–29
Ruban AV, Berera R, Ilioaia C, van Stokkum IHM, Kennis JTM, et al. 2007. Identification of a mechanism of photoprotective energy dissipation in higher plants. *Nature* 450:522–75
Ryan-Keogh TJ, Macey AI, Nielsdóttir MC, Lucas MI, Steigenberger SS, et al. 2013. Spatial and temporal development of phytoplankton iron stress in relation to bloom dynamics in the high-latitude North Atlantic Ocean. *Limnol. Oceanogr.* 58:533–45
Schallenberg C, Strzepek RF, Schuback N, Clementson LA, Boyd PW, et al. 2020. Diel quenching of Southern Ocean phytoplankton fluorescence is related to iron limitation. *Biogeosciences* 17:793–812
Schatz GH, Brock H, Holzwarth AR. 1988. Kinetic and energetic model for the primary processes in photosystem II. *Biophys. J.* 54:397–405
Schrader PS, Milligan AJ, Behrenfeld MJ. 2011. Surplus photosynthetic antennae complexes underlie diagnostics of iron limitation in a cyanobacterium. *PLOS ONE* 6:e18753
Schreiber U, Schliwa U, Bilger W. 1986. Continuous recording of photochemical and nonphotochemical chlorophyll fluorescence quenching with a new type of modulation fluorometer. *Photosynth. Res.* 10:51–62
Schuback N, Hoppe CJ, Tremblay JÉ, Maldonado MT, Tortell PD. 2017. Primary productivity and the coupling of photosynthetic electron transport and carbon fixation in the Arctic Ocean. *Limnol. Oceanogr.* 62:898–21

Schweitzer RH, Brudvig GW. 1997. Fluorescence quenching by chlorophyll cations in photosystem II. *Biochemistry* 36:11351–59

Sherman J, Gorbunov MY, Schofield O, Falkowski PG. 2020. Photosynthetic energy conversion efficiency along the West Antarctic Peninsula. *Limnol. Oceanogr.* 65:2912–25

Sidler WA. 1994. Phycobilisome and phycobiliprotein structures. In *The Molecular Biology of Cyanobacteria*, ed. DA Bryant, pp. 139–216. Dordrecht, Neth.: Kluwer Acad.

Stokes GG. 1852. On the change in the refrangibility of light. *Philos. Trans. R. Soc. Lond.* 142:463–562

Suggett DJ, Moore CM, Hickman AE, Geider RJ. 2009. Interpretation of fast repetition rate (FRR) fluorescence: signatures of phytoplankton community structure versus physiological state. *Mar. Ecol. Prog. Ser.* 376:1–19

Sunda WG, Huntsman SA. 1997. Interrelated influence of iron, light and cell size on marine phytoplankton growth. *Nature* 390:389–92

Vassiliev IR, Kolber ZS, Wyman KD, Mauzerall D, Shukla VK, et al. 1995. Effects of iron limitation on photosystem II composition and light utilization in *Dunaliella tertiolecta*. *Plant Physiol.* 109:963–72

Vernotte C, Etienne AL, Briantais JM. 1979. Quenching of the system II chlorophyll fluorescence by the plastoquinone pool. *Biochim. Biophys. Acta* 545:519–27

Wilson A, Ajlani G, Verbavatz JM, Vass I, Kerfeld CA, et al. 2006. A soluble carotenoid protein involved in phycobilisome-related energy dissipation in cyanobacteria. *Plant Cell* 18:992–1007

Wilson A, Boulay C, Wilde A, Kerfeld CA, Kirilovsky D. 2007. Light-induced energy dissipation in iron-starved cyanobacteria: roles of OCP and IsiA proteins. *Plant Cell* 19:656–72

Yamamoto HY. 1979. Biochemistry of the violaxanthin cycle in higher plants. *Pure Appl. Chem.* 51:639–48

Zhu Y, Ishizaka J, Tripathy SC, Wang S, Sukigara C, et al. 2017. Relationship between light, community composition and the electron requirement for carbon fixation in natural phytoplankton. *Mar. Ecol. Prog. Ser.* 580:83–100

Annual Review of Marine Science

Volume 14, 2022

Contents

Errata

An online log of corrections to *Annual Review of Marine Science* articles may be found at http://www.annualreviews.org/errata/marine